BioGecko

Vol 12 Issue 03 2023

ISSN NO: 2230-5807

Thermophoresis and Soret-Dufour Impacts on MHD Viscous Dissipative Micropolar Fluid Past an Inclined Isothermal Surface

P. Roja[1*], T. Sankar Reddy[2], M. Parvathi[3], P. Chandra Reddy[4], M. Umamaheswar[5]

[1,3,4,5]Deparment of Mathematics, Annamacharya Institute of Technology and sciences, Rajampeta, Kadapa-516126, A.P., India.*

[2] Department of Mathematics, Annamacharya Institute of Technology and sciences, C. K. Dinne, Kadapa-516003, A.P., India.

Corresponding Email: [1]rojasvu09@gmail.com*

Abstract

An analysis is presented to investigate thermophoresis and the combined effects of Soret and Dufour effects on Magnetohydrodynamic free convection heat and mass transfer flow of a micropolar fluid past an inclined isothermal plate in the presence of viscous dissipation with suction/injection and heat generation/ absorption and subject to the thermal radiation. The governing non linear partial differential equations of the problem are transformed into a system of nonlinear ordinary differential equations through appropriate similarity transformation and shooting technique method with Runge–Kutta Fourth order integration scheme. The effects of various physical parameters on the dimensionless velocity, microrotation, temperature, and concentration profiles are discussed and presented graphically. Finally, numerical values of the physical quantities, such as the local skin friction coefficient, the local Nusselt number and the local Sherwood number are tabulated with the variation of thermal Grashof number, modified Grashof number, magnetic parameter and coupling constant, radiation parameter, Eckert number, parameter thermophoretic parameter and Schmidt number parameters.

Keywords: Thermophoresis, MHD; Mass Transfer; Viscous Dissipation, Micropolar; Suction/injection; Heat Generation/Absorption.

1. INTRODUCTION

In last two decades, the theory of micropolar fluid has received enormous attentions, since the traditional Newtonian fluids cannot specifically depict the feature of fluid with suspended particles, polar fluids, suspension solutions, liquid crystals, colloidal solutions and fluid containing small additives. Physically, micropolar fluids may present the non-Newtonian fluids consisting of short rigid cylindrical elements or dumb-bell molecules, polymer fluids, fluids suspensions and animal blood. The existence of dust or smoke particular in a gas may also be modeled using micropolar fluid dynamics. Eringen [1] first derived the theory of micropolar fluids, which illustrates the microrotation effects to the microstructures. Eringen [2] extended his idea to the theory of thermomicropolar fluids, which interest to the special effects of

microstructures on the fluid flow. The mathematical theory of equations of micropolar fluids and applications of these fluids in the theory of lubrication and in the theory of porous media are given in recent books by Eringen [3] and Lukaszewicz [4].

Free convection in the boundary layer flow of a micropolar fluid along a vertical wavy surface was investigated by Chiu and Chou [5]. Hassanien and Gorla [6] studied the heat transfer to a micropolar fluid from a non-isothermal stretching sheet with suction and blowing. Mixed convection boundary layer flow of a micropolar fluid on a horizontal plate was derived by Gorla [7]. Furthermore, The flow characteristics of the boundary layer of micropolar fluid over a semi-infinite plate in different situations have been studied by many authors in Refs. [8–15]. In the above mentioned works the effect of the induced magnetic field was neglected.

The problem of natural convection-radiation interaction on boundary layer flow with Rosscland diffusion approximation along a vertical thin cylinder has been investigated by Hossain and Alim [16]. Hossain and Takhar [17] employed finite difference approximation to analyze the effects of conduction-radiation interaction on natural convection boundary layer flow of a viscous incompressible fluid along an isothermal horizontal plate. Abdel-naby *et al.* [18] studied the radiation effects on MHD unsteady free convection flow over a vertical plate with variable surface temperature. Hossain [19] analyzed the effect of viscous and Joule heating effects on MHD free convection flow with variable plate temperature. The heat generation effect on MHD natural convection flow along a vertical flat plate was studied by Mamun *et al.* [20] employing finite difference techniques. Palani and Kim [21] applied implicit finite difference scheme of Crank-Nicolson method to analyze the importance of Joule heating and viscous dissipation effects on MHD flow along inclined plate subject to variable surface temperature. In view of all publications MHD convective flow of micropolar fluid without thermophoresis. Recently, Rashed et al. [22] The coupled heat and mass transfer by mixed convection boundary layer flow of a micropolar fluid over a continuously moving isothermal vertical surface immersed in a thermally and solutal stratified medium have been investigated in the presence of chemical reaction effect.

Thermophoresis is an excellent phenomenon by which small sized particles suspended in a non-isothermal gas acquire a velocity relative to the gas in the direction of decreasing temperature. The velocity acquired by the particles is called thermophoretic velocity and the force experienced by the suspended particles due to the temperature gradient is known as thermophoretic force. Goren [23] was the first to study the role of thermophoresis in laminar flow of a viscous incompressible fluid. He used the classical problem of flow over a flat plate to calculate the deposition rates and showed that substantial changes in surface deposition can be obtained by increasing the difference between the surface and free stream temperature. Thermophoretic deposition of radioactive particles is considered to be one of the important

factors causing accidents in nuclear reactors. Epstein et .al. [24] investigated the thermophoretic transport of small particles through a free convection boundary layer adjacent to a cold, vertical deposition surface in a viscous incompressible fluid. Garg and Jayaraj [25] studied the thermophoretic transport of small particles in forced convection flow over an inclined plate. Opiolka et al. [26] analyzed the combined effects of electrophoresis and thermophoresis on particle deposition onto flat surface. The effect of surface mass transfer on mixed convection flow past a heated vertical flat permeable plate with thermophoresis was studied by Selim et al. [27]. Wang [28] discussed the combined effects of inertia and thermophoresis on particle deposition onto a wafer with wavy surface. Thermophoresis causes small particles to depositon cold surfaces. Alam al el. [29] examined the effects of variable suction and thermophoresis on steady MHD combined free-forced convective heat and mass transfer flow over a semi-infinite permeable inclined plate in the presence of thermal radiation. Duwairi and Damesh [30] investigated the effects of thermophoresis particle deposition on mixed convection from vertical surfaces embedded in saturated porous medium. Pakravan and Yaghoubi [31] investigated theoretically the combined thermophoresis, Brownian motion and Dufour effects on natural convection of nanofluids. Mehdi and Hosseinalipour [32] examined particle migration in nanofluids considering thermophoresis and its effect on convective heat transfer. Recently Anbuchezhian et.al., [33] have investigated thermophoresis and Brownian motion effects on boundary layer flow of nanofluid in the presence of thermal stratification due to solar energy. To our knowledge, there are no published results that include the effects of thermal radiation and viscous dissipation on MHD mixed convection flow of micropolar fluid in the presence of thermophoresis.

So far, most of previous works are not studied MHD free convective flow of micropolar fluid in the presence of the thermophoresis. In the present work we have considered the effect of viscous dissipation and heat generation/absorption on heat and mass transfer flow of a micro-polar fluid over an inclined isothermal plate in the presence of thermophoresis when the magnetic field is imposed transverse to the plate with suction/injection. Therefore, the objective of the present paper is to study the combined effects of thermal radiation, viscous dissipation and heat generation/absorption on steady Magnetohydrodynamic mixed convective heat and mass transfer flow of a viscous incompressible micropolar fluid past a an inclined radiative isothermal surface in the presence of thermophoresis.

2. Mathematical analysis:

Let us, consider a steady two-dimensional MHD convective flow of viscous incompressible electrically conducting micropolar fluid past an inclined radiative isothermal permeable surface with an acute angle a to the vertical with *x*-axis measured along the plate, a magnetic field of uniform strength B_0 is applied in the *y*-direction which is normal to the flow direction. Fluid suction is imposed at the plate surface and the suction hole size is taken to be constant. The temperature of the surface is held uniform at T_w which is higher than the ambient temperature T_∞ .The Rosseland approximation is used to describe the radioactive heat flux in the

x-direction which is considered negligible in comparison to the *y*-direction. The effects of thermophoresis are being taken into account to help in the understanding of the mass deposition variation on the surface. Under the above assumptions, the governing equations for this problem can be written as:

(i) Continuity:

$$\frac{\partial u}{\partial x}+\frac{\partial u}{\partial y}=0 \tag{1}$$

(ii) Momentum:

$$u\frac{\partial u}{\partial x}+v\frac{\partial u}{\partial y}=\nu\frac{\partial^2 u}{\partial y^2}+g\beta_T\left(T-T_\infty\right)cos\alpha+g\beta_C\left(C-C_\infty\right)cos\alpha$$
$$+K_1\frac{\partial N}{\partial y}-\frac{\sigma B_0{}^2}{\rho}u \tag{2}$$

(iii) Angular momentum:

$$G_1\frac{\partial^2 N}{\partial y^2}-2N-\frac{\partial u}{\partial y}=0 \tag{3}$$

(vi) Energy:

$$u\frac{\partial T}{\partial x}+v\frac{\partial T}{\partial y}=\frac{k}{\rho c_p}\frac{\partial^2 T}{\partial y^2}-\frac{1}{\rho c_p}\frac{\partial q_r}{\partial y}+\frac{\nu}{c_p}\left(\frac{\partial u}{\partial y}\right)^2+\frac{Q_0}{\rho c_p}(T-T_\infty) \tag{4}$$

(v) Concentration:

$$u\frac{\partial C}{\partial x}+v\frac{\partial C}{\partial y}=D\frac{\partial^2 C}{\partial y^2}-\frac{\partial}{\partial y}(V_T C) \tag{5}$$

where u and v are the velocity components in the *x*, y directions, ν is the kinematic viscosity, g is the acceleration due to gravity, β_T and β_C are the coefficient of thermal and volumetric expansions , respectively, T, is the temperature of thermal boundary layer fluid , T_w is the wall temperature of the inclined plate, T_∞ is the temperature far away from the plate, C_w is the wall concentration of the solute , C_∞ is the concentration of the solute far away from the sheet. σ is the electrical conductivity, B_0 is the magnetic induction, λ is the fluid thermal conductivity, ρ is the fluid density, C_p is the specific heat at constant pressure, q_r is the radiative heat flux in the y-direction, Q_0 is the heat generation (>0) or absorption (<0) coefficient , μ is the dynamic viscosity, D is the molecular diffusivity of the species concentration and V_T is the thermophoretic velocity.

The boundary conditions for the model are as follows

$$u = U_0,\ v = \pm v_w(x),\ N = -\frac{1}{2}\frac{\partial u}{\partial y},\ T = T_w,\ C = C_w, at\ y = 0 \qquad (6)$$
$$u \to U_\infty,\ N \to 0,\ T \to T_\infty,\ C \to C_\infty,\ \text{as}\ y \to \infty$$

where U_0 is the uniform plate velocity and $v_w(x)$ represents fluid mass suction or injection on the porous surface. The transpiration function variable $v_w(x)$ of order $x^{-1/2}$ 1/2 is considered.

By using the Rosseland approximation, the radiative heat flux in the y' direction is given by

$$q_r = -\frac{4\sigma_1}{3k_1}\frac{\partial T^4}{\partial Y} \qquad (7)$$

where σ_1 is the Stefan-Boltzmann constant and k_1 is the mean absorption coefficient.

Assuming that the temperature differences within the flow are sufficiently small so that T^4 can be expanded in Taylor series about the free stream temperature T_∞ to yield

$$T^4 \cong 4T_\infty^3 T - 3T_\infty^4 \qquad (8)$$

where the higher-order terms of the expansion are neglected.
By using (6) and (7), Eq. (4) gives

$$u\frac{\partial T}{\partial x} + v\frac{\partial T}{\partial y} = \frac{k_e}{\rho c_p}\frac{\partial^2 T}{\partial y^2} - \frac{16\sigma T_\infty^3}{3\rho c_p k_1}\frac{\partial^2 u}{\partial y^2} + \frac{\nu}{c_p}\left(\frac{\partial u}{\partial y}\right)^2 + \frac{Q_0}{\rho c_p}(T - T_\infty) \qquad (9)$$

The second, third and fourth on the RHS of the Eq. (9) denote the thermal radiation, viscous dissipation and Jjoule heating terms, respectively.

Now the thermophoretic velocity V_T , which appears in the Eq. (4) can be written as [23]:

$$V_T = -kv\frac{\nabla T}{T_{ref}} = \frac{-kv}{T_{ref}}\frac{\partial T}{\partial y} \qquad (10)$$

where T_{ref} is a reference temperature and k is the thermophoretic coefficient with range of value from 0.2 to 1.2 as

$$k = \frac{2Cs\left(\lambda_g/\lambda_p + C_t K_n\right)\left[1 + K_n\left(C_1 + C_2 e^{-C_3/K_n}\right)\right]}{\left(1 + 3C_m K_n\right)\left(1 + 2\lambda_g/\lambda_p + 2C_t K_n\right)} \qquad (11)$$

where C_1, C_2, C_3, C_m, C_s, C_t are constants, λ_g and λ_p are the thermal conductivities of the fluid and diffused particles respectively and K_n is the Knudsen number.

A thermophoretic parameter τ can be defined as follows:

$$\tau = \frac{-k\left(T_w - T_\infty\right)}{T_r} \qquad (12)$$

Typical values of τ are 0.01, 0.05 and 0.1 corresponding to approximate values of $-k\left(T_w - T_\infty\right)$ equal to 3K, 15K and 30 K for a reference temperature of $T_r = 300K$.

3. Similarity transformation

The solutions of the governing equations are obtained by introducing the following non-dimensional variables:

$$\eta = \left(\frac{U_0}{2\nu x}\right)^{1/2} y,\ \psi = \left(2\nu U_0 x\right)^{1/2} f(\eta),\ \theta(\eta) = \frac{T - T_\infty}{T_w - T_\infty},\ \phi(\eta) = \frac{C - C_\infty}{C_w - C_\infty},$$
$$u = U_0\, f'(\eta),\ v = -\sqrt{\frac{2\nu U_0}{x}}\left[f(\eta) - \eta f'(\eta)\right],\ N = \left(\frac{U_0}{2\nu x}\right)^{1/2} U_0 g(n) \quad (13)$$

If the dimensional stream function $\psi(x, y)$ then $u = \frac{\partial \psi}{\partial y}$ and $u = -\frac{\partial \psi}{\partial x}$.

The continuity equation is automatically satisfied and the system of Eqs. (2), (3), (5) and (9) becomes:

$$f''' + ff'' - Mf' + Gr\,\theta\cos\alpha + Gc\,\phi\cos\alpha + Kg' = 0 \quad (14)$$
$$Gg'' - 2(2g + f'') = 0 \quad (15)$$
$$(3R + 4)\theta'' + 3R\,\mathrm{Pr}\, f\theta' + 3R\,\mathrm{Pr}\, Ec(f'')^2 + = 0 \quad (16)$$
$$\phi'' + Sc(f - \tau\theta')\phi' - Sc\tau\theta''\phi = 0 \quad (17)$$

The primes mean differentiation with respect to η, $M = \left(\frac{\sigma U_\infty}{\rho}\right)^{1/2} B_0$ is the is the magnetic field parameter, $G = \frac{G_1 U_0}{2\nu x}$ is the micro-rotation parameter, $Gr = \frac{g\beta_T\left(T_w - T_\infty\right)2x}{U_0{}^2}$ is the local thermal Grashof number, $Gc = \frac{g\beta_c\left(C_w - C_\infty\right)2x}{U_0{}^2}$ is the local solute Grashof number, $K = \frac{K_1}{\nu}$ is the coupling parameter, $\mathrm{Pr} = \frac{\nu}{K}$ is the Prandtl number, $R = \frac{kk_e}{4\sigma_s T_\infty^3}$ is the thermal radiation parameter, $Ec = \frac{U_0^2}{c_p\left(T_w - T_\infty\right)}$ is the Eckert number, $Q = \frac{Q_0}{\rho c_p}$ is the heat aborption parameter, $Sc = \frac{\nu}{D}$ is the Schmidt number, $\tau = -\frac{k\left(T_w - T_\infty\right)}{T_r}$ is the thermoporesis parameter.

The transformed boundary conditions (6) are given by

$$f(0)=f_w,\ f'(0)=1,\ g(0)=-\frac{1}{2}f''(0),\ \theta(0)=1,\ \phi(0)=1$$
$$f(\infty)=0,\ g(\infty)=0,\ \theta(\infty)=0,\ \phi(\infty)=0 \quad (18)$$

Where $f_w=-v_w(x)\sqrt{\frac{2x}{\upsilon U_0}}$ is the s the dimensionless wall mass transfer coefficient such that $f_w>0$ denotes wall suction and $f_w<0$ denotes wall injection.

The physical quantities of interest are the local skin friction coefficient, the wall heat transfer coefficient (or the local Nusselt number) and the wall deposition flux (or the local Stanton number) which are defined as respectively where the skin friction coefficient C_f, the couple stress coefficient C_m, the heat transfer $q_w(x)$ and the mass transfer Sh_x from the wall are given by

$$C_f\,\mathrm{Re}_x^{-1/2}=\frac{\tau_w}{(1/2)\rho U_o^2}=2f''(0),\ \tau_w=\mu\left(\frac{du}{dy}\right)_{y=0} \quad (19)$$

From the temperature field, we can study the rate of heat transfer which is given by

$$Nu_x\,\mathrm{Re}_x^{-1/2}\left(\frac{3R}{3R+4}\right)=\frac{q_w(x)}{\lambda\left(T_w-T_\infty\right)}=-\frac{1}{2}\theta'(0);q_w(x)=-\lambda\left(\frac{\partial T}{\partial y}\right)_{y=0}-\frac{4\sigma}{3k_1}\left(\frac{\partial T^4}{\partial y}\right)_{y=0} \quad (20)$$

From the concentration field, we can study the rate of mass transfer which is given by

$$Sh_xSt\,\mathrm{Re}_x^{-1/2}=-\frac{J_s}{U_0C_\infty};J_s=-D\left(\frac{\partial C}{\partial y}\right)_{y=0}=\phi'(0) \quad (21)$$

where $\mathrm{Re}_x=U_0x/\nu$ the local Reynolds number.

3. Method of solution:

The system of ordinary differential Eqs. (14) – (17) subject to the boundary conditions (18) are solved numerically using Runge–Kutta fourth-order integration with shooting iteration technique. A step size of $\Delta\eta=0.01$ was selected to be satisfactory for a convergence criterion of 10^{-6} in all cases. The results are presented graphically in Figs. 1–10 and conclusions are drawn for flow field and other physical quantities of interest that have significant effects.

4. Results and discussion

The Eqs. (11)–(13) constitute highly non-linear coupled boundary value problem of third and second order. Thus we have used the shooting iteration technique with Runge–Kutta fourth-order integration algorithm. For numerical results we considered the non dimensional parameter

values as fw =0.2, *M* =1.0, *K*=0.1, *Gr=2.0*, *Gc=2.0*, *G=2.0*, *Pr=0.71*, *Ec=0.1*, *R=1.0* and *Sc* = 0.2. These values are kept as constant in entire study except the varied parameters as shown in figures 1–10 and Tables 1-2.. The results obtained shows the influences of the non dimensional governing parameters, namely magnetic field parameter, thermal and solutal Grashof numbers, coupling parameter, radiation parameter, thermophoretic parameter and the chemical reaction parameter on velocity, microratation, temperature and concentration profiles

The effect of the angle of inclination α on the velocity, microrotation, temperature and concentration profiles are shown in Figs 1(a)-(d), respectively. From Fig. 1(a) , the velocity profiles decrease with increasing values of angle of inclination. It is also seen Fig. 1(b) that the microrotation increases near the plate and then decreases far away from the plate as angle of inclination increases. From Figs. 1(c)-(d) it is observed that both thermal as well as concentration increases as angle of inclination increases.

Figs.2(a)-(d), respectively, illustrate the velocity, microrotation, temperature and concentration profiles for different values of suction parameter fw. From Fig. 2(a) , the velocity profiles decrease with increasing in suction parameter. It is also observed Fig. 2(b) that the microrotation increases near the plate and then decreases far away from the plate as suction parameter increases. From Figs. 2(c)-(d) we observed that both thermal as well as concentration decreases as suction parameter increases.

The effect of the magnetic parameter *M* on the velocity, microrotation and temperature profiles are shown in Figs 3(a)-(c), respectively. It is clearly seem From Fig. 1(a) that the velocity profiles decrease with increasing values of magnetic parameter. It is also seen Fig. 3(b) that the microrotation increases near the plate and then decreases far away from the plate as angle of inclination increases. In addition, from Figs. 3(c)-(d) it is observed that both thermal as well as concentration increases as magnetic parameter increases.

The velocity and microrotation profiles for different values of thermal Grashof number *Gr* and solutal Grashof number *Gc* are displayed in Figs. 4 and 5, respectively. It is observed that an increasing in *Gr* or *Gc* leads to increasing in the values of velocity whereas microrotation decreases near the plate and then increases far away from the plate.

For different values of coupling constant *K* on the velocity and microrotation profiles are presented in Figs. 6(a)-(b). It is found that velocity increases when the coupling constant is increased (See Fig. 6(a)). The results also show that the microrotation on the isothermal plate increases near the plate and opposite trends far away from the plate as coupling constant increases.

For different values of thermophoretic parameter τ on the velocity, microrotation and concentration profiles are plotted in Figs. 7(a)-(c). It is noticed that velocity increases with the increasing values of thermophoretic parameter. The results also show that the microrotation on

the isothermal plate increases near the plate and opposite trends far away from the plate as R increases. From Fig.7(c) it is clear that the concentration profile increases with increase of the radiation parameter.

Figs. 8(a)-(c) respectively, show the velocity and microrotation, temperature and concentration profiles for different values of Eckert number *Ec*. It is observed that velocity increases with the increasing values of Eckert number *Ec*. The results also show that the microrotation on the isothermal plate increases near the plate and opposite trends far away from the plate as Eckert number *Ec* increases. It is also seem Fig. 8(c) that temperature profiles increase with increase in Eckert number.

For different values of thermal radiation parameter *R*, the velocity and microrotation profiles are plotted in Fig. 9. It is obvious that velocity distribution across the boundary layer increases with the increasing values of radition parameter *R*. The results also show that the microrotation on the isothermal plate increases near the plate and opposite trends far away from the plate as R increases. From Fig.9(c) we see that the temperature profiles decrease with increase of the radiation parameter *R*.

The effects of various values of Schmidt number *Sc* on the velocity and microrotation profiles are presented in Fig. 10. It is shown that the translational velocity across the boundary layer increases with an increasing of *Sc*. Also, it is appear that the microrotation increases near the plate and opposite trends far away from the plate as *Sc* increases.

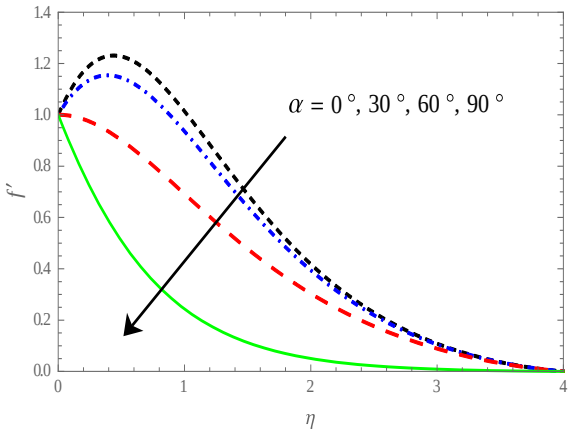

Fig 1(a). Effects of α on velocity distribution $f'(\eta)$

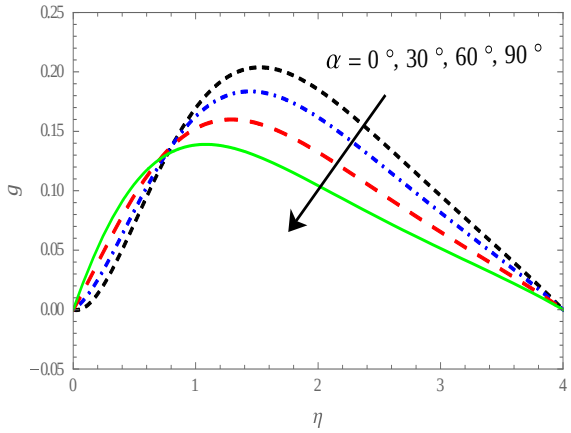

Fig 1(b). Effects of α on microrotation distribution $g(\eta)$

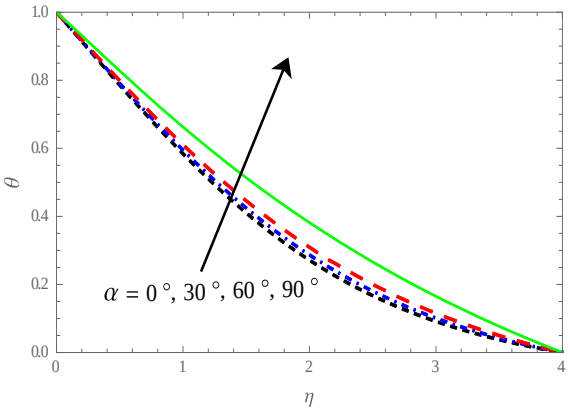

Fig 1(c). Effects of α on Temperature distribution $\theta(\eta)$

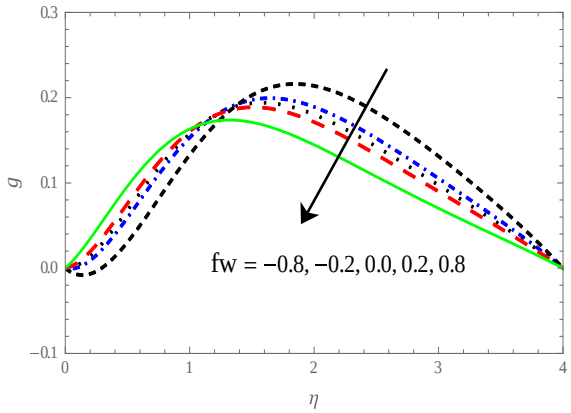

Fig 2(b). Effects of fw on Microrotation distribution g(η)

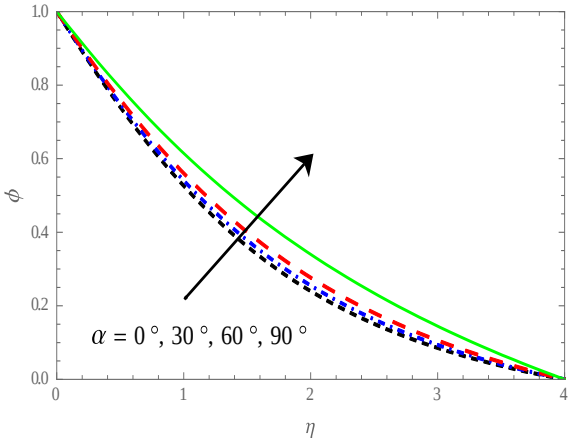

Fig 1(d). Effect of α on concentration distribution $\phi(\eta)$

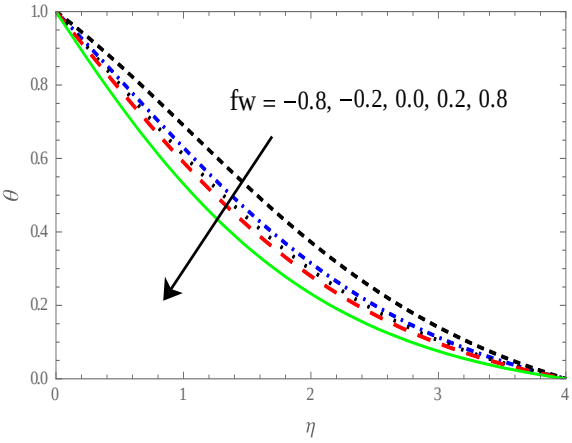

Fig 2(c). Effects of fw on temperature distribution $\theta(\eta)$

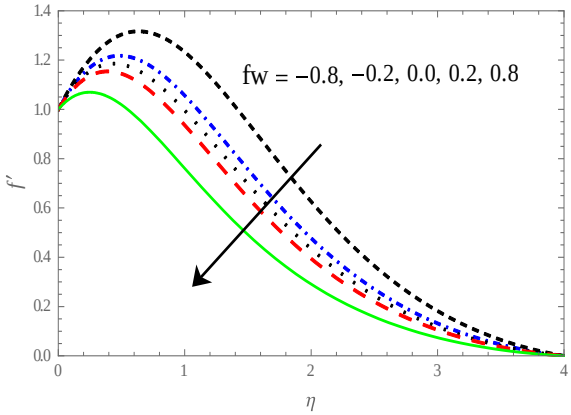

Fig 2(a). Effects of fw on velocity distribution $f'(\eta)$

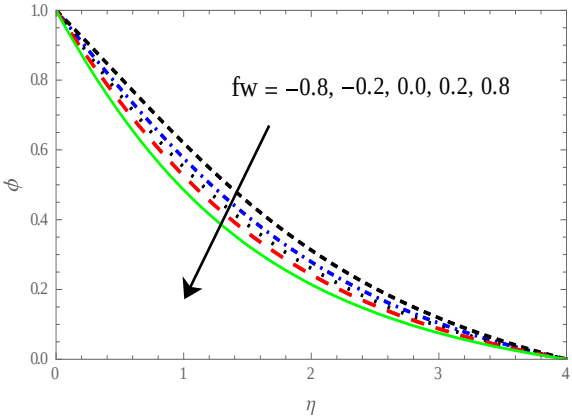

Fig 2(d). Effects of fw on concentration distribution $\phi(\eta)$

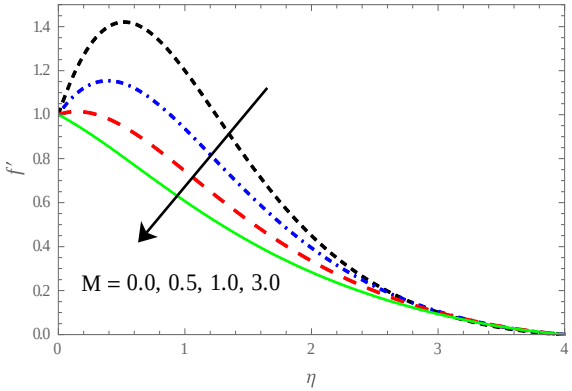

Fig 3(a). Effects of M on Velocity distribution $f'(\eta)$

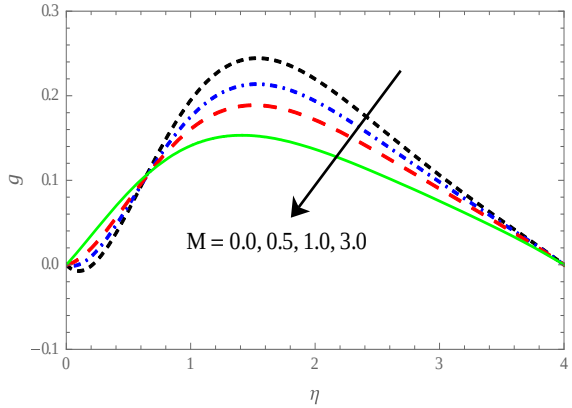

Fig 3(b). Effects of M on microrotation distribution $g(\eta)$

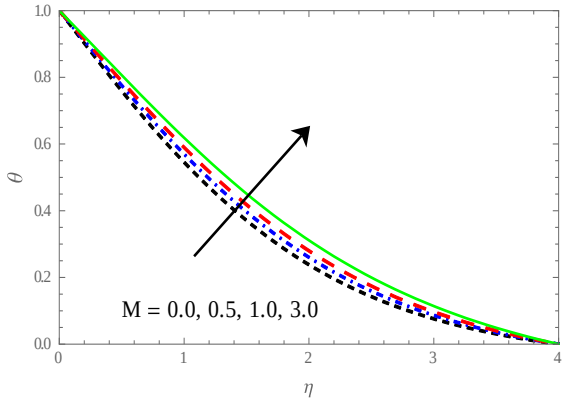

Fig 3(c). Effects of M on temperature distribution $\theta(\eta)$

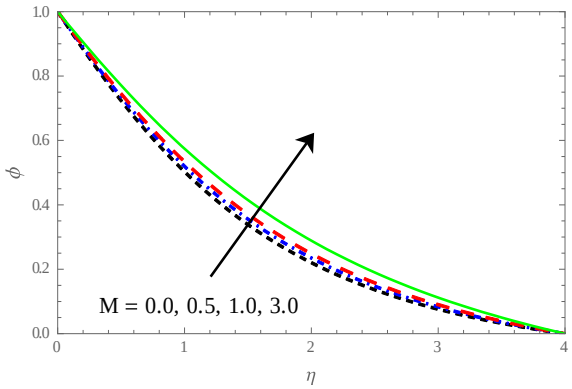

Fig 3(d). Effects of M on concentration distribution $\phi(\eta)$

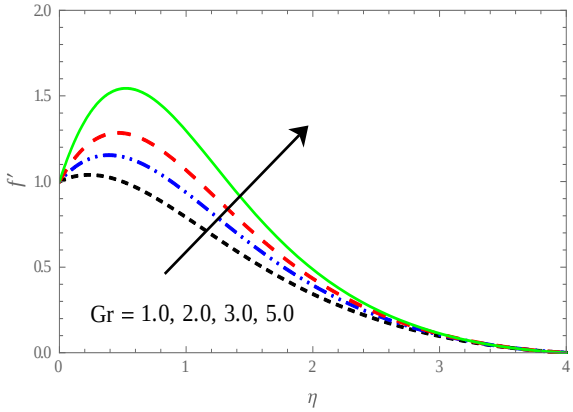

Fig 4(a). Effects of Gr on velocity distribution $f'(\eta)$

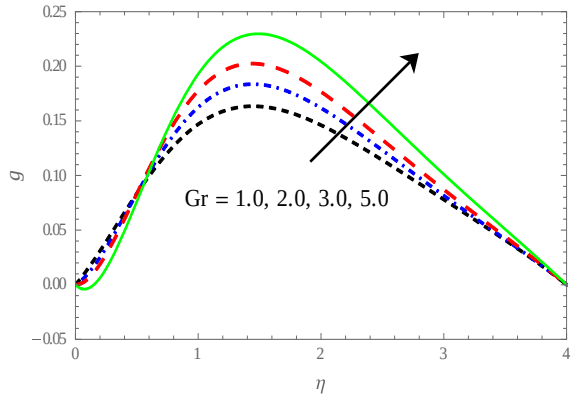

Fig 4(b). Effects of Gr on microrotation distribution $g(\eta)$

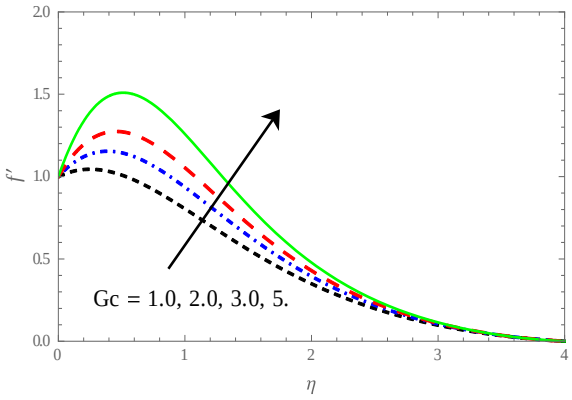

Fig 5(a). Effects of Gc on velocity distribution $f'(\eta)$

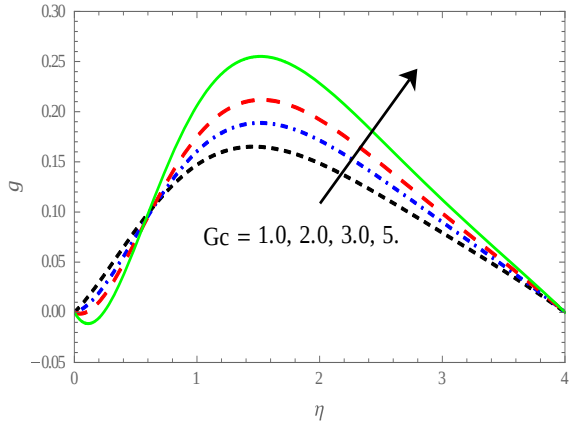

Fig 5(b). Effects of Gc on microrotation distribution $g(\eta)$

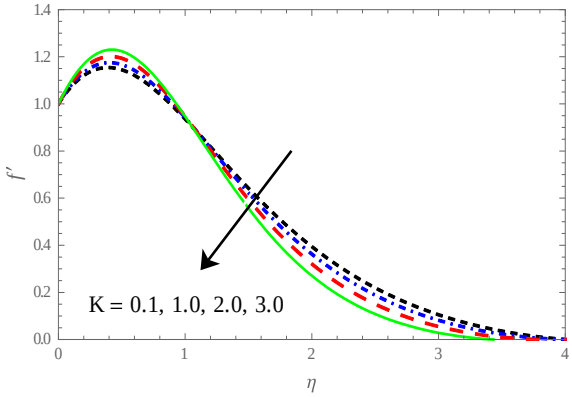

Fig 6(a). Effects of K on velocity distribution $f'(\eta)$

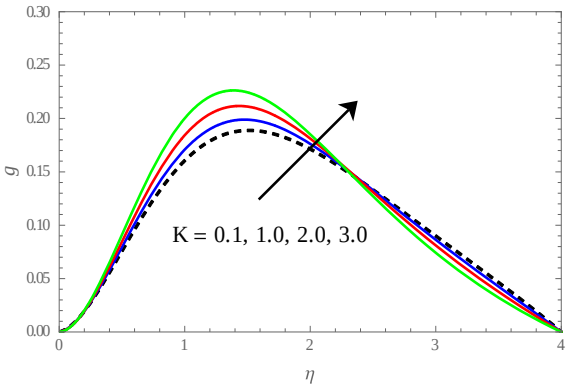

Fig 6(b). Effects of K on microrotation distribution $g(\eta)$

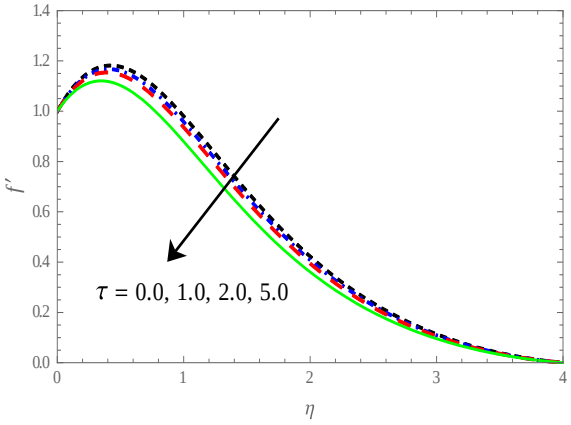

Fig 7(a). Effects of τ on velocity distribution $f'(\eta)$

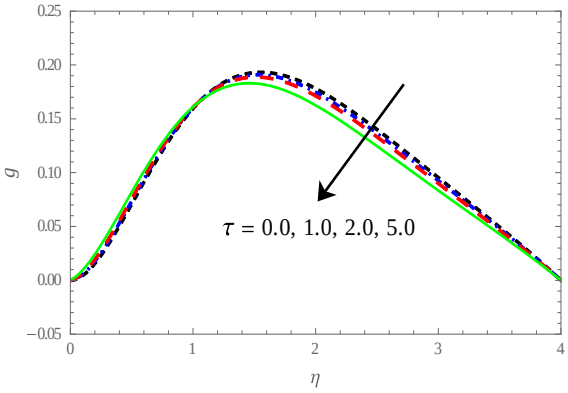

Fig 7(b). Effects of τ on microrotation distribution $g(\eta)$

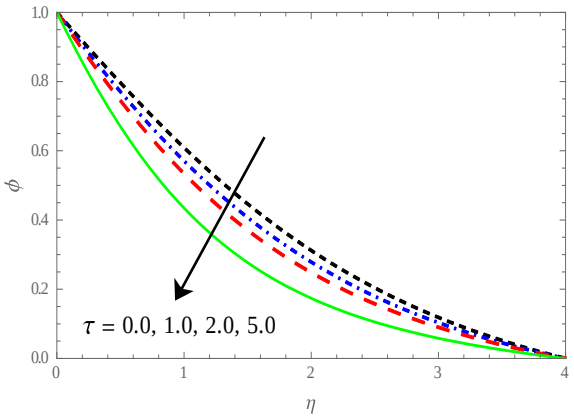

Fig 7(c). Effects of τ concentration distribution $g(\eta)$

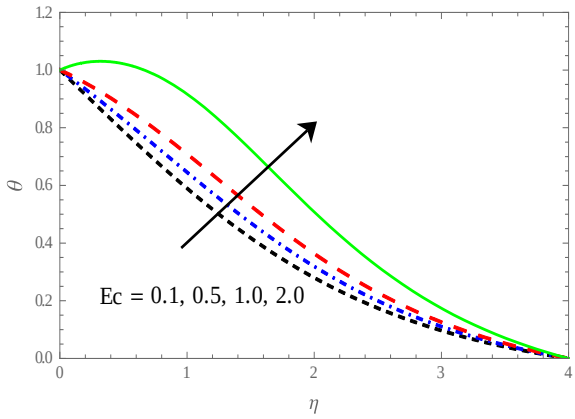

Fig 8(c). Effects of Ec temperature distribution $\theta(\eta)$

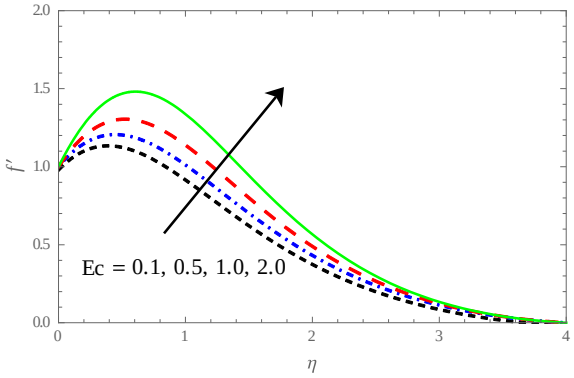

Fig 8(a). Effects of Ec on velocity distribution $f'(\eta)$

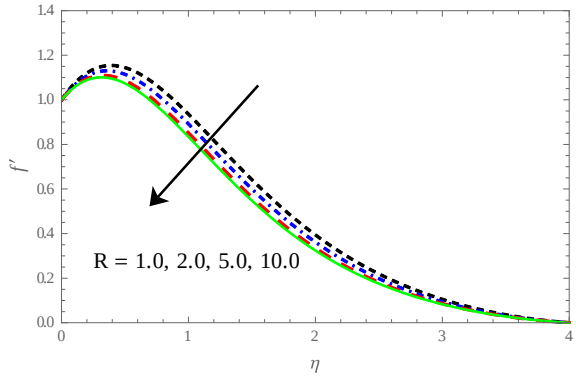

Fig 9(a). Effects of R on velocity distribution $f'(\eta)$

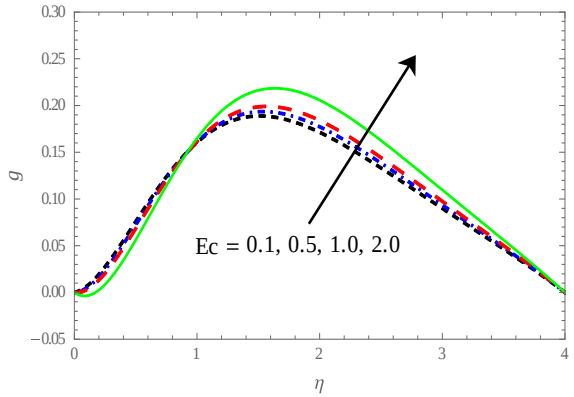

Fig 8(b). Effects of Ec on microrotation distribution $g(\eta)$

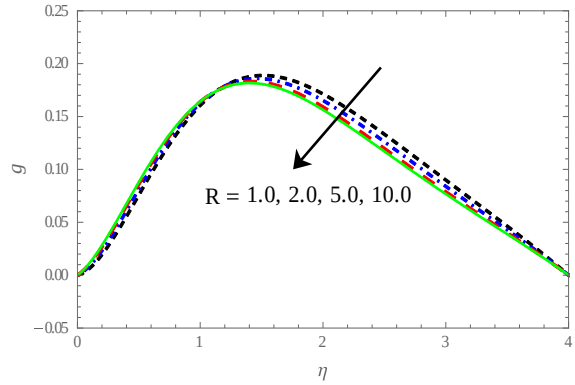

Fig 9(b). Effects of R on microrotation distribution $g(\eta)$

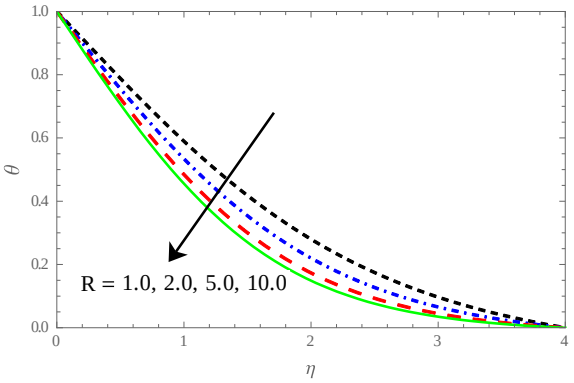

Fig 9(c). Effects of R on temperature distribution $\theta(\eta)$

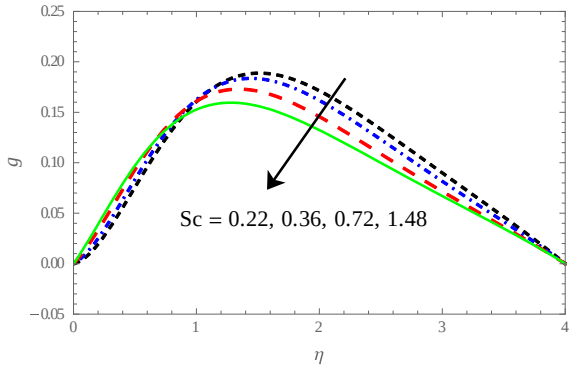

Fig 10(b). Effects of Sc on microrotation distribution g(η)

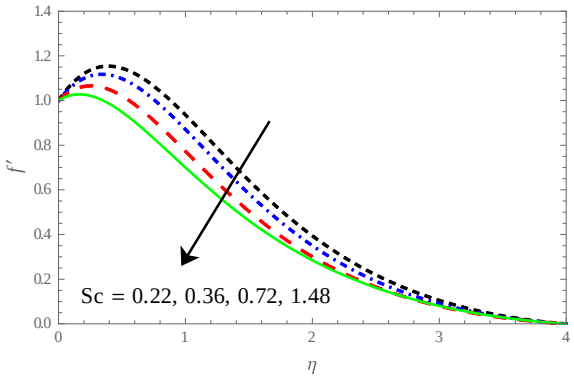

Fig 10 (a). Effects of Sc on velocity distribution $f'(\eta)$

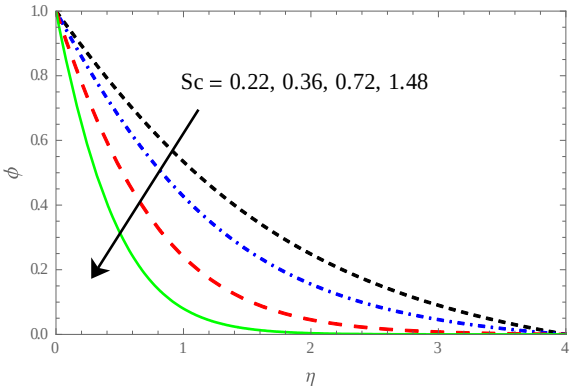

Fig 10(c). Effects Sc of on concentration distribution $\theta(\eta)$

The values of skin-friction coefficient, local Nusselt number and local Stanton number are tabulated in Tables 1-2 for various values of thermal Grashof number *Gr*, modified Grashof number *Gc*, magnetic parameter M and coupling constant *K*, Radiation parameter, Eckert number Ec, thermophoretic parameter τ and Schmidt number. It is clear that from Table 1the values of the skin-friction coefficient, local Nusselt number numerically increase with increase in the thermal Grashof number and modified Grashof number and coupling constant, while they decreases with increasing magnetic parameter. It is also found that the local Nusselt number decreases as increase thermal Grashof number and modified Grashof number and coupling constant. In addition, from Table 2, we observe that increase the values of radiation parameter *R*, Eckert number Ec, thermophoretic parameter τ and Schmidt number *Sc* decrease in the values of skin-friction coefficient and local Stanton number, while increase in local Nusselt number by increasing in the values of Eckert number, thermophoretic parameter and Schmidt number.

Table 1 Variations in skin-friction coefficient, local Nusselt number and local Stanton number for different parameters for $\alpha = 30^0$, G=2.0, R=1.0, Ec=0.1, $\tau = 2.0$, Sc=0.22, Pr=0.71.

Gr	Gc	M	K	C_f	Nu_x	Sh_x
2.0				1.14773	0.427590	0.555509
3.0				1.703161	0.423660	0.571029
5.0				2.75175	0.415802	0.592628
	2.0			1.14773	0.427590	0.555509
	3.0			1.16720	0.421598	0.569727
	5.0			2.67711	0.418125	0.589552
		0.5		1.565882	0.455373	0.579184
		1.0		1.147731	0.427590	0.555509
		3.0		1.128582	0.368161	0.502163
			0.1	1.147732	0.427590	0.555509
			1.0	1.223312	0.425791	0.555505
			2.0	1.315751	0.422981	0.555503

Table 2 Value of skin-friction coefficient, local Nusselt number and local Stanton number for different parameters for $\alpha = 30^0$, G=2.0, Pr=0.71 , Gr= Gc=2.0 M=1.0 and K=0.1.

R	Ec	τ	Sc	C_f	Nu_x	Sh_x
1.0				1.147732	0.427590	0.555509
2.0				1.067781	0.498186	0.577004
5.0				1.029362	0.534942	0.588731
	0.1			1.147735	0.427590	0.555509
	0.3			1.235952	0.299285	0.509175
	0.5			1.338162	0.149012	0.455137

	1.0		1.189622	0.428641	0.489146
	2.0		1.147731	0.427590	0.555509
	3.0		1.107661	0.426549	0.624089
		0.22	1.147732	0.427590	0.555509
		0.30	1.021182	0.423624	0.747992
		0.48	1.015261	0.421152	0.868317

4. Conclusion:

The combined effects of thermal radiation and viscous dissipation on MHD mixed convection heat and mass transfer flow of a micropolar fluid past an inclined isothermal permeable surface due to the effects of thermophoresis are investigated.
From the present investigation, the following conclusions are drawn:

- The velocity decreases with increase in angle of inclination α, suction parameter fw magnetic parameter *M*, coupling constant *K*, thermophoresis parameter τ, radiation parameter *R* and Schmidt number *Sc Sc* whereas increases with increase thermal Grashof number *Gr*, modified Grashof number *Gc* and Eckert number *Ec*.
- The microrotation increase near the surface and then decrease far away from the surface with increase in angle of inclination α, suction parameter fw, magnetic parameter *M*, coupling constant *K*, radiation parameter *R*, thermophoresis parameter τ, Eckert number *Ec* and Schmidt number *Sc* whereas increases with increase thermal Grashof number *Gr*, modified Grashof number *Gc* and Eckert number *Ec*.
- The Temperature increases with increase in angle of inclination α, magnetic parameter *M* and Eckert number *Ec* whereas decreases with increasing in radiation parameter *R*.
- The concentration increases with increase in angle of inclination α and magnetic parameter *M* whereas decreases with increasing in thermophoresis parameter τ and Schmidt number *Sc*.
- Both the Skin friction coefficient and rate of mass transfer increases with increase in *Gr, Gc, K* and *Ec* leads to rise an increase in the but they decrease for the values of *M*, τ ,*R* and *Sc*.
- Increasing thermal Grashof number *Gr*, modified Grashof number *Gc*, coupling constant *K*, Eckert number *Ec*, thermophoresis parameter τ and *Sc*, the rate of heat transfer decreases whereas it decreases as magnetic parameter *M* increases.

5. References

[1]. Eringen AC. Theory of micropolar fluids. J Math Mech. (1966);16:1–18.
[2]. Eringen AC. Theory of thermomicropolar fluids. J Math Anal Appl. (1972);38:480–96.

[3]. Eringen AC. Microcontinuum field theories II: fluent media. New York: Springer; 2001.
[4]. Lukaszewicz G. Micropolar fluids: theory and applications. Basel: Birkhauser; 1999.
[5]. Chiu C.P and Chou H.M., Free convection in the boundary layer flow of a micropolar fluid along a vertical wavy surface, Acta Mech. 101 (1993) 161–174.
[6]. Hassanien I.A., Gorla R.S.R., Heat transfer to a micropolar fluid from a non-isothermal strething sheet with suction and blowing, Acta Mech. 84 (1990) 191–199.
[7]. Gorla R.S.R, Mixed convection boundary layer flow of a micropolar fluid on a horizontal plate, Acta Mech. 108 (1995) 101–109.
[8]. Ahmadi G., Self-similar solution of incompressible micropolar boundary layer flow over a semi-infinite plate, Int. J. Eng. Sci. 14 (1976) 639–646.
[9]. Gorla R.S.R., Pender R., Eppich J., Heat transfer in micropolar boundary layer flow over a flat plate, Int. J. Eng. Sci. 19 (1983) 1431–1439.
[10]. Soundalgekar V.M, Takhar H.S, Flow of micropolar fluid past a continuously moving plate, Int. J. Eng. Sci. 21 (1983) 961–965.
[11]. Takhar H.S., Soundalgekar V.M., Flow and heat transfer of micropolar fluid past a porous plate, Indian. J. Pure Appl. Math. 16 (5) (1985) 552–558.
[12]. Hassanien I.A., Gorla R.S.R., Heat transfer to a micropolar fluid from a non-isothermal stretching sheet with suction and blowing, Acta Mech. 84 (1990) 191–199.
[13]. Takhar H.S., Agarwal R.S., Bhargava R., Jain S., Mixed convection flow of a micropolar fluid over a stretching sheet, Heat Mass Transfer 34 (1998) 213–219.
[14]. Mansour M.A., Gorla R.S.R., Micropolar fluid flow past a continuously moving plate in the presence of magnetic field, Appl. Mech. Eng. 4 (1999) 663–672.
[15]. Mansour M.A., Mohammadein A.A., El-Kabeir S.M.M., Gorla R.S.R., Heat transfer from moving surface in a micropolar fluid, Can. J. Phys. 77 (1999) 463–471.
[16]. Hossain M. A and Alim M. A., 1997. Natural convection-radiation interaction on boundary layer flow along a thin vertical cylinder, Journal of Heat and Mass Transfer 32, p. 515-520.
[17]. Hossain M. A and Takhar H. S., 1999. Thermal radiation effects on natural convection flow over an isothermal horizontal plate, Heat and Mass Transfer 35, p. 321-326.
[18]. Abd El-Naby M. A., Elsayed M. E. Elbarbary and Nader Y. Abdelazem, 2003. Finite difference solution of radiation effects on MHD unsteady free convection flow over vertical plate with variable surface temperature, Journal of Applied Mathematics 2003, 2, p.65-86.
[19]. Hossain M. A., 1992. Viscous and Joule heating effects on MHD free convection flow with variable surface temperature, International Journal of Heat and Mass Transfer 35, p.3485-3487.
[20]. Mamun A. A, Chowdhury Z. R, Azim M. A. and Molla M. M., 2008. MHD-conjugate heat transfer analysis for a vertical flat plate in presence of viscous dissipation and heat

generation, International Journal Communications in Heat and Mass Transfer 35, p. 1275-1280.

[21]. Palani G. And Kwang Young Kim, 2011. Joule heating and viscous dissipation effects on MHD flow past a semi-infinite inclined plate with variable surface temperature, Journal of Engineering Thermophysics 20, p. 501-517.

[22]. Rashad A.M, Abbasbandy S, Chamkha A.J, Mixed convection flow of a micropolar fluid over a continuously moving vertical surface immersed in a thermally and solutally stratified medium with chemical reaction 2016 *J. Taiwan Int. of . chemical engineers*, 45, pp.2163-2169.

[23]. Goren SL. Thermophoresis of aerosol particles in laminar boundary layer on flat plate. *J Colloid Inter face Sci* 1977; 61: 77–85.

[24]. Epstein M, Hauser GM, Henry RE. Thermophoretic deposition of particles in natural convection flow from vertical plate. *ASME J Heat Trans,* 1985; 107: 272–276.

[25]. Garg VK, Jayaraj S. Thermophoresis of aerosol particles in laminar flow over inclined plates. *Int J Heat Mass Trans,* 1988; 31: 875–890.

[26]. Opiolka S, Schmidt F, Fissan H. Combined effects of electrophoresis and thermophoresis onparticle deposition onto flat surfaces. *J. Aerosol Sci.,* 1994; 25: 665–671.

[27]. Selim A, Hossain MA, Rees DAS. The effect of surface mass transfer on mixed convection flow past a heated vertical flat permeable plate with thermophoresis. *Int J Thermal Sci* 2003; 42: 973–982.

[28]. Wang C.C. Combined effects of inertia and thermophoresis on particle deposition onto a wafer with wavy surface. *Int. J. Heat Mass Trans.* 2006; 49:1395–1402.

[29]. Alam MS, Rahman MM, Sattar MA. Effects of variable suction and thermophoresis on steady MHD combined free-forced convective heat and mass transfer flow over a semi-infinite permeable inclined plate in the presence of thermal radiation. *Int J Thermal Sci.* 47 (2008)758–765.

[30]. Duwairi H. M., Damesh R. A. Effects of thermophoresis particle deposition on mixed convection from vertical surfaces embedded in saturated porous medium, *Int. J. Numer. Meth. Heat Fluid Flow*, (2008) 18(2), 202-216.

[31]. Pakravan H.A, Yaghoubi M, Combined thermophoresis, Brownian motion and Dufour effects on natural convection of nanofluids, *Int. J. Therm. Sci.,* 50 (2011) 394–402.

[32]. Mehdi B, Hosseinalipour S.M., Particle migration in nanofluids considering thermophoresis and its effect on convective heat transfer, *Thermo. chim. Acta* 574 (2013) 47–54.

[33]. Anbuchezhian N, Srinivasan N, Chandrasekaran K, Kandasamy R, Thermophoresis and Brownian motion effects on boundary layer flow of nanofluid in presence of thermal stratification due to solar energy, *Appl. Math. Mech.,* 33(6) (2012) 765–780.